Basis Set Effects on the Stabilities and Interaction Energies of Small Amide Molecules Adsorbed on Kaolinite Surface

Najwa-Alyani Mohd Nabil[1], Lee Sin Ang[1*], and Shukri Sulaiman[2]

[1]*Faculty of Applied Sciences, Universiti Teknologi MARA, Perlis Branch, Arau 02600, Malaysia*

[2]*School of Distance Education, Universiti Sains Malaysia, Pulau Pinang 11800, Malaysia*

** **Corresponding author:***

email: anglee631@uitm.edu.my

Received: December 6, 2022
Accepted: May 19, 2023

DOI: 10.22146/ijc.79795

Abstract: *Adsorptions of small amide molecules, acetamide (AA) and* N*-methyl-acetamide (NMA) on the surface of kaolinite are investigated in this study. The focus is on the basis set effects towards the stabilities and the interaction energies of the molecules on the Al–O surface. With a fixed B3LYP functional, we increased the size of the basis sets for the single-point calculations, to find the converged interaction energies and obtain the relative stabilities. We found that, under the direct usage of Pople-type and Dunning's correlation consistent basis sets, it is not possible to achieve the pattern of convergence for the interaction energies and the relative stabilities. Compared to the complete basis set (CBS) extrapolation scheme, the double zeta basis sets deviated the most, in the range of 21 to 27%, while it is from 1 to 7% for the triple zeta basis sets. Based on the results, we suggest using 6-311++G(2df,2pd) or cc-pVQZ for energy-related quantities. Compared to AA, NMA attached more strongly by 0.5 eV on the surface of Al–O.*

Keywords: *adsorption; amide molecules; basis set; density functional theory; kaolinite*

■ INTRODUCTION

Basis sets are the wavefunctions for individual atoms. Its importance cannot be overstated as it forms the basis of quantum chemical calculations. The wavefunction of molecular systems is usually obtained under the linear combination of atomic orbitals (LCAO), especially those density-based and *ab initio* calculations. The accuracy of a wavefunction depends on the quality of the basis sets [1-2]. Consensus stated that the larger the basis set, the better the wavefunction [3]. With this notion, calculations are usually performed at the largest basis set that the computational resources can afford [4]. However, this does not guarantee that the basis set used is adequate for the work being done. The better-quality work is always the one where the calculation is supposed to be calculated with the next higher basis set, which infuses uncertainty into the results of the current work.

This brings to the topic of basis set convergence, which is an aspect of calculations that needed to be addressed [5-6]. The obtained values from calculations with increasing sizes of basis sets will be stopped only when the changes to the values are below a certain threshold. A direct way to deal with the basis set convergence is by systematically increasing the size of the basis set and adding polarization and diffusion functions [7]. However, the approach is not straightforward as it is difficult to find basis sets that are defined beyond a certain size, not to mention that the calculations to be performed will need enormous computer resources. Another approach is by using extrapolation schemes, known as complete basis set (CBS) [8-10]. Even though it is applied primarily to the wavefunction-based method, complete basis set calculations have also been used to extrapolate the structural and frequencies at the limit of the DFT at the B3LYP level [11-14]. However, the size of the systems investigated consisted only of small molecules. Conveniently, an online calculator has been set up to calculate the extrapolated values from different schemes [15]. CBS is also a well-known approach to overcome the incompleteness of basis sets.

One of the important calculations in theoretical work is to find the strength of an interaction between

components. It is also used as a check on the stability of systems. For example, the adsorption of molecules on surfaces (e.g., graphene, boron nitride, metals, and clay). Theoretical approaches used to study the interactions include the cluster and periodic calculations, under a variety of approximations, either quantum mechanical, Monte Carlo, or force fields [16-18]. The interactions between constituent molecules of a system have a few names to them. Interaction energy (also known as the adsorption energy) and binding energy have been used to show the strength of the interaction between constituents as Eq. (1). Using a supermolecular approach, the interaction energy (E_{int}) and binding energy (E_{bin}) can be calculated by:

$$E_{int} \text{ or } E_{bin} = E_{complex\ AB} - E_{monomer\ A} - E_{monomer\ B} \quad (1)$$

The difference between E_{int} and E_{bin} is the way the energies of the monomers are obtained. For E_{int}, the energies of the monomers are "calculated at the same positions of the nuclei as those in the total system", while for E_{bin}, the nuclei of the monomers are at their optimal positions [19-20]. However, some research papers do not seem to separate clearly these two quantities.

Previously, adsorption of the amide molecules has been performed [21-24]. However, the reported relative stability for formamide (FA), acetamide (AA), *N*-methylformamide (NMFA), and *N*-methylacetamide (NMA) absorbed on the kaolinite surfaces have been inconsistent with different basis sets [24], which may be rectified by considering the basis sets effects. In this project, we investigate the differences between the two systems in terms of interaction energy and relative stability. The focus is on the adsorption of amide molecules on kaolinite surfaces. Two smallest amide molecules, AA and NMA were selected for the investigations, as we would like to keep computational resources within a manageable range. Also, both molecules were investigated in a previous report [24], which enables comparisons to be made. We show that the strength of the interaction between the kaolinite surface and the amide molecules is dependent on the basis sets used and found that one should not conclude on the relative stability of an adsorption study based on the results of a single basis set. Finally, we suggested basis sets to be used for the investigation of interaction energies and relative stability in amides absorbed on the Al–O surface.

■ EXPERIMENTAL SECTION

Materials

The Al–O kaolinite surface is modeled from the crystal structure of kaolinite by Bish et al. [25]. Only the octahedral surface is used as it can form stronger interactions with adsorbates, as compared to the tetrahedral [21,26], hence easier to obtain converged structures. The final octahedral (001) surface cluster has 6 silicone atoms, 6 aluminum atoms, 36 oxygen atoms, and 23 hydrogen atoms. For the initial positions of the AA and NMA molecules, both vertical and horizontal orientations of the amide molecules on the surface of the Al–O are considered (the molecules are shown in Fig. 1).

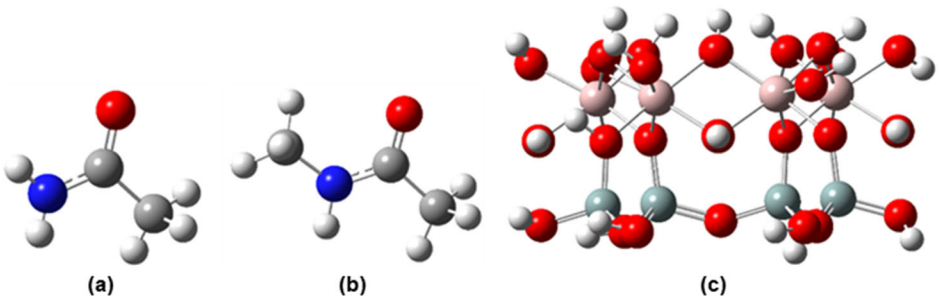

Fig 1. The structures used in this investigation: (a) acetamide (AA), (b) *N*-methyl-acetamide (NMA), (c) model of Al–O. Red sphere represents oxygen, blue represents the nitrogen, grey represents the silicon, peach represents the aluminium. For clarity, in the subsequent figures, the closest surface to the AA and NMA is the Al–O surface

Procedure

Geometry relaxations were performed at the basis 6-31G* and 6-31G**, to gauge the effects of adding polarization functions to the hydrogen atoms. Only the hydrogen and the oxygen atoms closest to the amide molecules are relaxed, together with the amide molecules. All the quantum mechanical calculations in this work were performed with the G09 suite of program [27], and the analyses on the wavefunction by Multiwfn [28]. The renderings of the figures in the work were done with GaussView [29] and UCSF ChimeraX [30]. With the geometry obtained at 6-31G*, and later re-optimized at 6-31G**, single point calculations using larger size basis sets were performed with split-valence (6-311++G** and 6-311++G(2df,2pd)) and Dunning's correlation-consistent (cc-pVDZ, cc-pVTZ, and cc-pVQZ) basis sets. The number of basis functions for the AA and NMA is shown in Table 1. With 505 and 513 electrons in the system of AA and NMA, respectively, the smallest number of the basis functions is 884, while the largest is 3863.

Using the B3LYP functional, we set out to find the changes in the interaction energies of the attachment of the amide molecules on the Al–O kaolinite surface. B3LYP is omnipresent in the molecular studies, making this level of theory a standard across many fields of study. Semi-empirical dispersion corrections of GD3BJ were included in the calculations of the interaction energies. Eq. (1) is used in the calculations of the strength of the interactions between adsorbates and Al–O surface.

Table 1. Number of basis functions in the calculations

Basis sets	System	
	AA	NMA
6-31G*	884	903
6-31G**	968	993
6-311++G**	1436	1472
6-311++G(2df,2pd)	2284	2348
cc-pVDZ	916	940
cc-pVTZ	2000	2058
cc-pVQZ	3748	3863

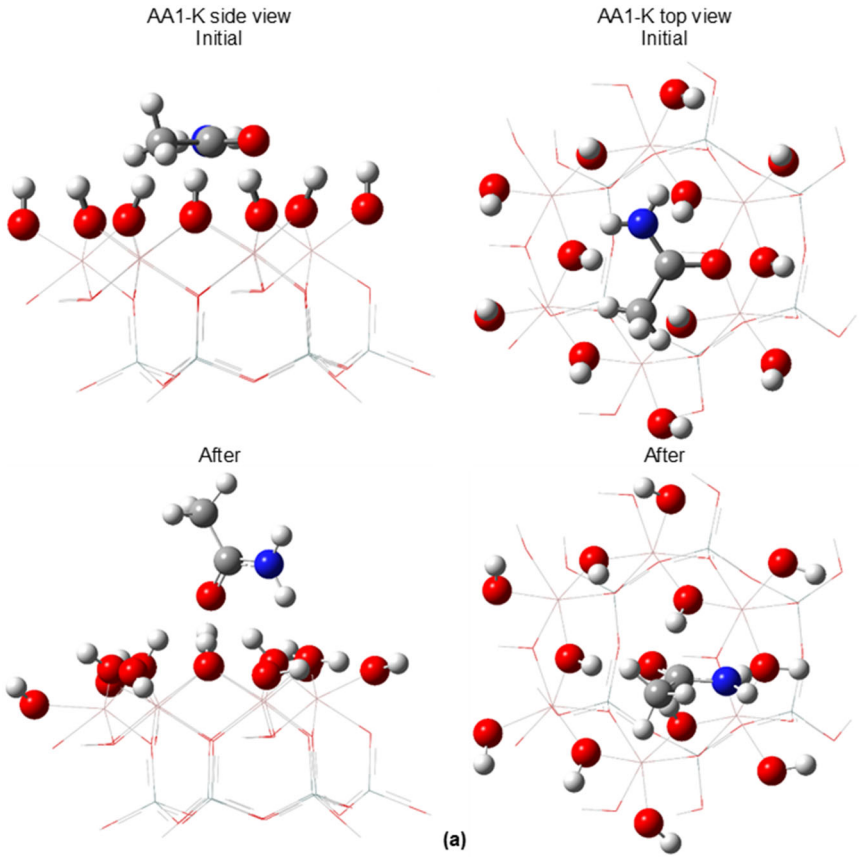

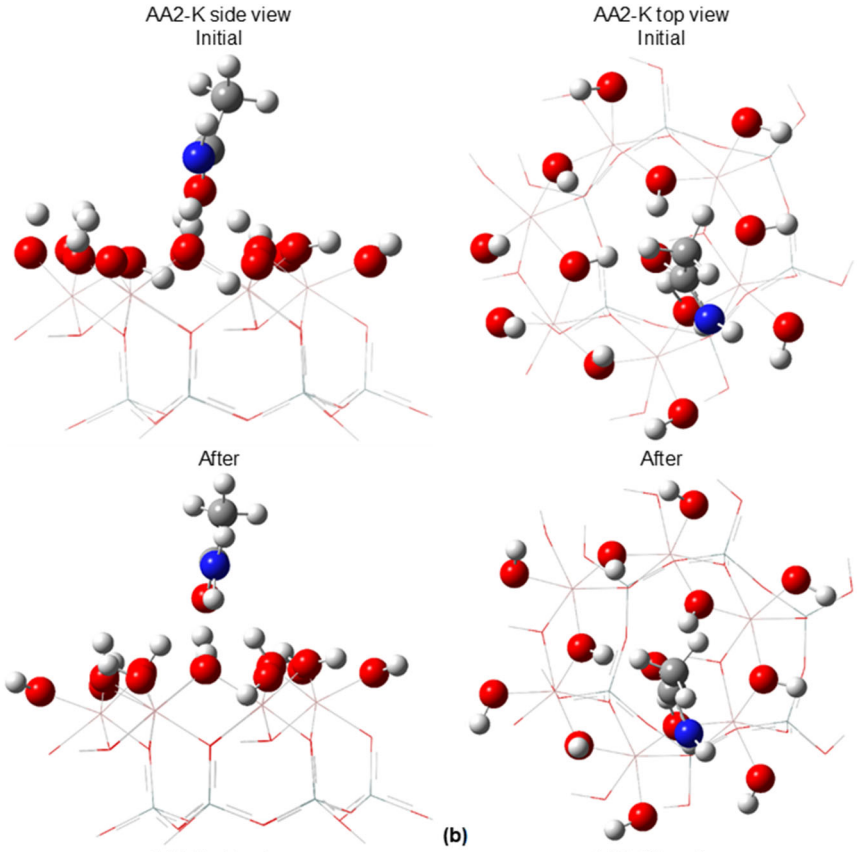
AA2-K side view
Initial
AA2-K top view
Initial
After
After
(b)
AA3-K side view
Initial
AA3-K top view
Initial
After
After
(c)

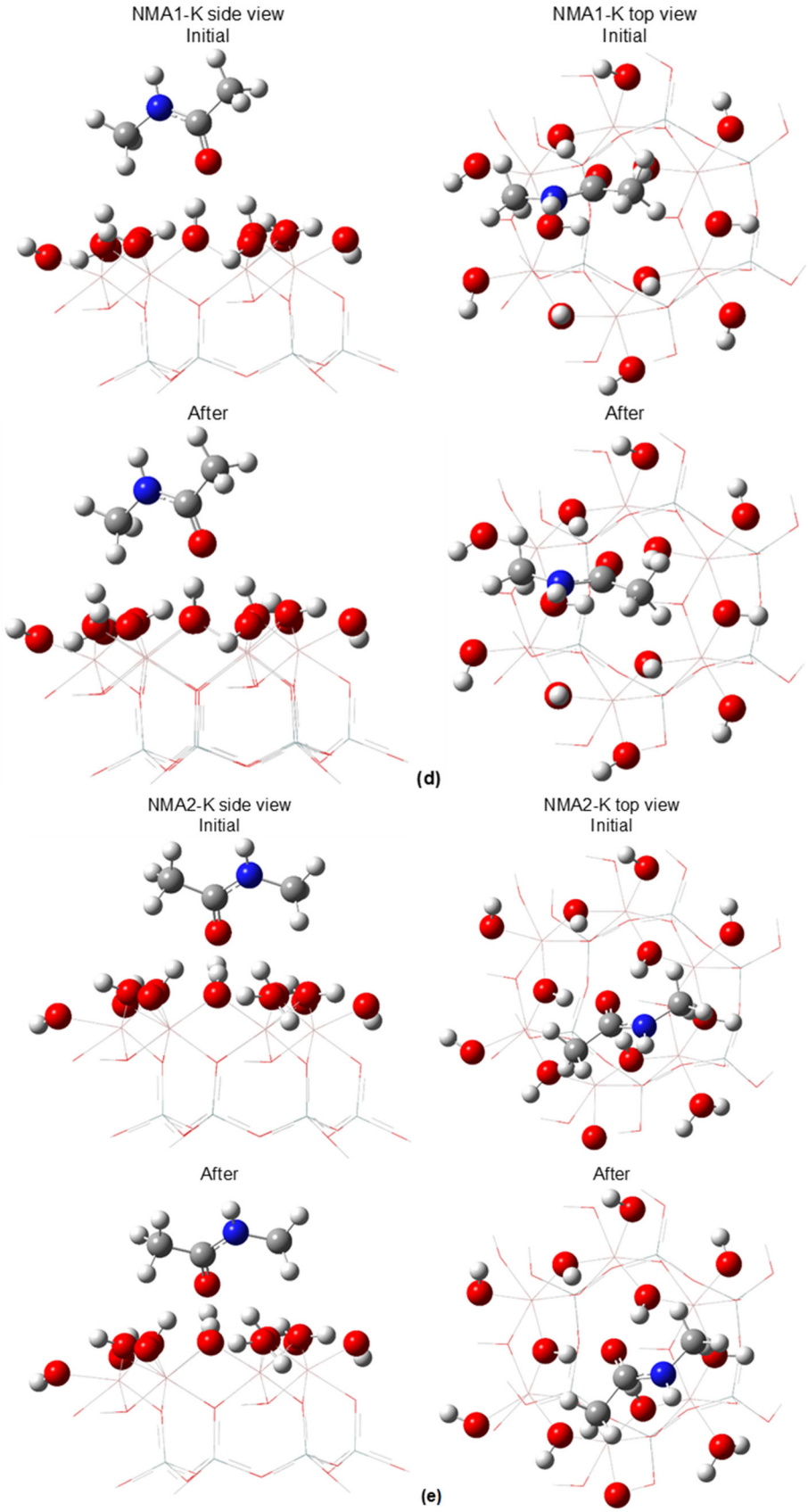
NMA1-K side view
Initial
NMA1-K top view
Initial
After
After
(d)
NMA2-K side view
Initial
NMA2-K top view
Initial
After
After
(e)

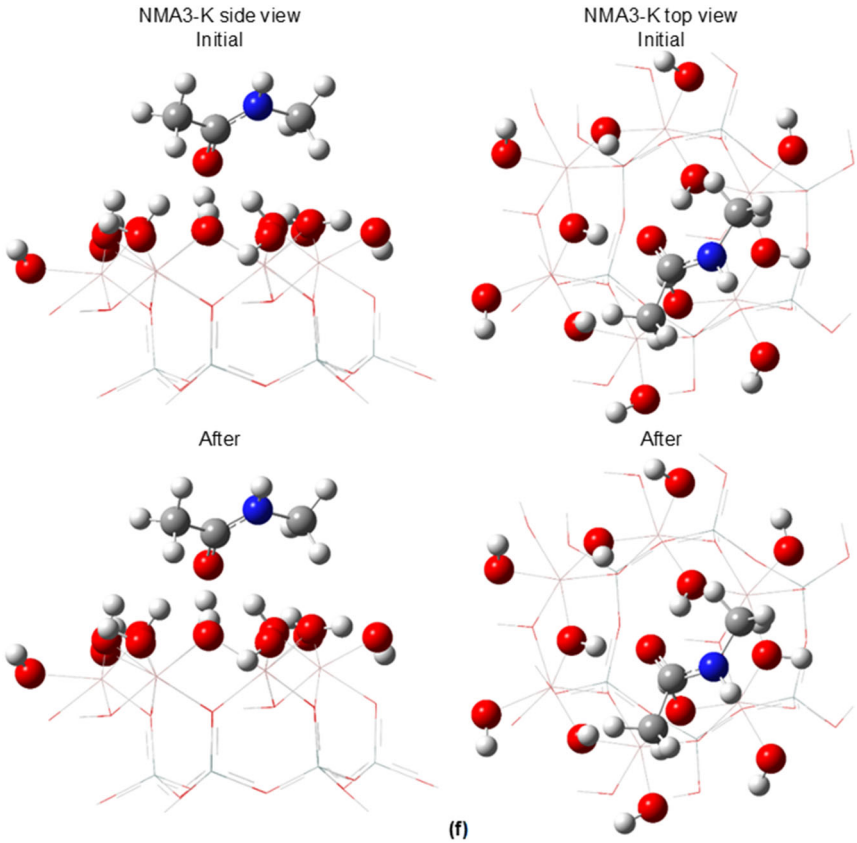

Fig 2. The initial and optimized structures of AAi-K ((a) to (c)) and NMAi-K ((d) to (f)) cluster I, where i = 1, 2, 3

■ RESULTS AND DISCUSSION

The resultant geometries as relaxed using the B3LYP/6-31G** method, which are shown in Fig. 2. The atoms shown in spheres were relaxed, while the ones in the wireframe were fixed. With the initial orientations of either planar or vertical, the AA and NMA molecules were found to always move to vertical or oblique orientations. The preferred orientation common in all cases is where the oxygen of the AA and NMA is directed toward the surface of the Al–O. This orientation is similar to the geometries obtained for water and acetic acid [26] and formamide [21], and hydrogen bondings are observed. For AA (Fig. 2(a) to (c)), the $-NH_3$ is found to be closer to the surface, and $-CH_3$ pointing up. For NMA, in Fig. 2(d), the $-NH-CH_3$ is found to be closer to the Al–O surface than the $-CH_3$ side alone. This behavior changes in Fig. 2(e) and 2(f), where there is no significant difference between the two side moieties as to which side is preferable to the Al–O surface.

The distances between the atoms in AA and NMA to Al–O are given in Tables 2 and 3. The O80 and O72 are the oxygens from AA and NMA, respectively. The other oxygens in Tables 2 and 3 are the Al–O surface oxygens, each attached to a hydrogen. These O–H are relaxed. For the AA molecule, AA3 system has the shortest and largest distances between O80 and the hydrogen on the surface of Al–O (1.770 Å with H33 and 3.066 Å with H56), while the corresponding values for AA1 and AA2 systems are in between these two extremes. For the NMA molecule, O72 has the shortest distance with hydrogen at 1.765 Å (in NMA3 system), and the longest at 3.746 Å (in NMA1 system). Within the three systems, NMA2 and NMA3 have the NMA molecule closer to the surface of Al–O (in which their average O72···H is shorter than in NMA1).

As for the O–H on the Al–O surface, the distances for the three systems are between 0.963 and 0.977 Å for AA, and between 0.961 and 0.976 Å for NMA. These values, using B3LYP/6-31G**, do not deviate much from

Table 2. The distances between atoms in the relaxed structure for AA systems

Selected atom pairs		Distances in systems (Å)		
Atom 1	Atom 2	AA1	AA2	AA3
O80	H33	1.792	1.835	**1.770**
O80	H45	1.902	1.992	1.798
O80	H56	2.976	2.848	3.066
O80	H61	2.062	1.772	1.920
O4	H14	0.975	0.973	0.976
O12	H13	0.975	0.972	0.972
O17	H18	0.972	0.965	0.969
O23	H45	0.972	0.965	0.969
O24	H33	0.977	0.970	0.972
O27	H28	0.972	0.968	0.970
O36	H37	0.974	0.971	0.970
O40	H56	0.968	0.965	0.964
O48	H49	0.974	0.970	0.968
O51	H57	0.965	0.964	0.963
O60	H61	0.971	0.976	0.967
O63	H64	0.974	0.971	0.970

Table 3. The distances between atoms in the relaxed structure for NMA systems

Selected atom pairs		Distances in systems (Å)		
Atom 1	Atom 2	NMA1	NMA2	NMA3
O72	H33	1.860	1.785	**1.765**
O72	H45	3.746	1.960	1.955
O72	H56	1.899	2.823	2.955
O72	H61	2.425	1.785	1.890
O4	H14	0.975	0.968	0.976
O12	H13	0.976	0.975	0.975
O17	H18	0.966	0.968	0.967
O23	H45	0.961	0.966	0.965
O24	H33	0.968	0.971	0.972
O27	H28	0.967	0.969	0.970
O36	H37	0.971	0.970	0.970
O40	H56	0.974	0.965	0.965
O48	H49	0.968	–	0.968
O51	H57	0.962	0.964	0.962
O60	H61	0.967	0.976	0.971
O63	H64	0.969	0.970	0.970

the O–H bond lengths reported in the adsorption of urea on kaolinite, but underestimated the experimental values from Bish [25]. This observation shows that the impact on the O–H bond length of the cluster for the adsorption of AA and NMA is similar to that of urea, possibly due to the similar fashion in AA and NMA react to the Al–O surface.

The distance of oxygen from AA to the hydrogen on the kaolinite surface, as reported by Song et al. [24] ranged from 1.906 to 2.305 Å, using B3LYP/6-31G*. In the same report, for the case of NMA, Song et al. [24] obtained 1.807 to 2.983 Å. Using a larger basis set (6-31G**) does produce a shorter and larger distance between the adsorbate and the surface. As the difference between the reported results [24] and this report in obtaining geometry is the polarization function added to hydrogen (6-31G* versus 6-31G**), it is interesting to check the effects on the larger basis sets on the geometrical relaxations. The result (Tables 2 and 3) where NMA moved closer to the kaolinite surface compared to AA, agrees with the result reported by Song et al. [24].

Further analysis of the depth of the molecules being absorbed on the Al–O surface was done by calculating the distance of O80 and O72 to the centroid of the seven aluminum atoms. This centroid was chosen because the aluminum atoms are the closest fixed atoms to the O80 or O72. It was found that AA3 and NMA2 are closest to the centroid, which means the two systems penetrated further than the other systems studied. NMA1 is displaced the furthest, compared to NMA2 and NMA3. The values are shown in Table 4.

For the stability, the relative energy (the difference in energy between the most stable to the other systems) is used. The relative energy gives insight into how strong the whole system is. While the total energy of the systems increases as the basis set increases in size (double zeta, triple zeta, quadruple zeta, and adding diffuse functions, as in Table 1), as required in the variational principle, the energies of the components also followed this trend: the

Table 4. Distance of the closest oxygen of AA (O80) and NMA (O72) to the centroid of the kaolinite cluster

System	Distance of O80 or O72 to centroid (Å)
AA1	3.024
AA2	3.038
AA3	2.913
NMA1	3.573
NMA2	2.903
NMA3	2.954

energy of kaolinite model and the amides increased with the basis sets. This observation applies to the Pople and Dunning's correlation-consistent basis sets. In Table 5, the relative energy shows that AA1 and NMA2 are the most stable systems. This observation is valid across the basis sets and the extrapolated values. Using the relative energy as a stability indicator, for acetamide, the ranking has it that AA1 is the most stable, followed by AA3 and AA2: AA1 > AA3 > AA2. For NMA, the stability has the order of NMA2 > NMA3 > NMA1. Hence, based on the relative energy, AA1 is the most stable system, while for the larger amide, NMA2 is the most stable system. As the orientation of the amides to the surface of kaolinite are all in a similar fashion (vertical or oblique), the lowest stability of AA2 and NMA1 can be attributed to the lack of penetration onto the surface of kaolinite, as mentioned in the optimized geometries.

To obtain the strength of the interaction between the components, the interaction energies are sought by using Eq. (1). The interaction energies are tabulated in Table 6. For the interaction energy of the AA-kaolinite systems, the strongest interaction is AA3 for the basis 6-31G** to cc-pVQZ, except for cc-pVDZ. However, although the total energies and the energies of the components increased as the basis sets becomes larger, the interaction energies are not always increasing accordingly. This is observed in the NMA-kaolinite systems: it increased in NMA1 and fluctuated in NMA2. But for the other systems, it decreased and is believed to converge to a constant value. The fluctuation in the interaction energy might be due to the non-uniform decrease in the total energy as the basis sets became larger.

As in the relative stability, CBS extrapolation has also been performed on the interaction energies. Referring to header CBS in Table 6, among the AA-kaolinite systems, AA3 possesses the strongest interaction, which is the same pattern observed for other basis sets (Pople's and Dunning's, except for cc-pVDZ). For AA3, the extrapolated value of –1.77 eV agrees well with the values obtained from triple-zeta and above basis sets (in Pople and Dunnings' basis sets), where the percentage difference from those values ranges from 1 to 7%. In comparison, the interaction energy for AA3, of 6-31G** and cc-pVDZ (the double zeta basis sets used in this study) deviated 21 and 27% respectively from those CBS values. Our CBS values are higher than the values

Table 5. Relative energy based on the total energy between the systems. The system with the most negative total energy is taken as the reference energy. The unit of the energy is eV

	6-31G** (geom. opt.)	6-311++G**	6-311++G(2df,2pd)	cc-pVDZ	cc-pVTZ	cc-pVQZ	CBS (exp)
AA1	0.00	0.00	0.00	0.00	0.00	0.00	0.00
AA2	0.94	1.09	1.15	1.10	1.15	1.59	1.93
AA3	0.11	0.13	0.11	0.07	0.10	0.11	0.12
NMA1	1.20	1.35	1.16	1.78	1.68	0.91	0.26
NMA2	0.00	0.00	0.00	0.00	0.00	0.00	0.00
NMA3	0.36	0.33	0.02	0.13	0.03	0.03	0.05

Table 6. Interaction energy of the AA and NMA from using Eq. (1). The unit of the energy is eV

	6-31G** (geom. opt.)	6-311++G**	6-311++G(2df,2pd)	cc-pVDZ	cc-pVTZ	cc-pVQZ	CBS (exp)
AA1	−1.93	−1.70	−1.63	−1.94	−1.66	−1.60	−1.58
AA2	−1.82	−1.59	−1.52	−2.25	−1.55	−1.07	−0.78
AA3	−2.14	−1.89	−1.81	−2.15	−1.84	−1.78	−1.77
NMA1	−1.27	−1.09	−1.02	−0.48	−0.54	−1.76	−2.76
NMA2	−2.82	−2.59	−2.27	−2.61	−1.70	−2.27	−2.73
NMA3	−1.98	−1.74	−1.67	−1.99	−1.69	−1.62	−1.60

shown by Song et al. [24] for the AA-kaolinite, in which their value is 0.39 eV. However, the magnitude of the interaction obtained here agree with the other hydrogen-bonded systems, for example, in the systems involving water molecule [31]. For the NMA-kaolinite systems, the fluctuations in the interaction energy from cc-pVDZ, cc-pVTZ, and cc-pVQZ render the CBS extrapolated values unreliable. Furthermore, the distance of O72 to the centroid for NMA1 is the furthest of the three positions, hence the interaction should not be the highest. The only trend that is acceptable is for NMA3, in which the CBS extrapolated value of –1.60 eV makes the interaction energy at 6-311++G(2df,2pd) 4% higher (–1.67 eV versus –1.60 eV). The comparison of CBS extrapolation and 6-311++G(2df,2pd) of AA2 is to be neglected, on the argument that the cc-pVDZ, cc-pVTZ and cc-pVQZ deviated too much from those of Pople basis sets. As can be seen from Table 6, the interaction energies from 6-311++G(2df,2pd) are all overestimated from the CBS extrapolated values, between 2.5 to 4.2%. Thus, the CBS extrapolated values for NMA2 should be lower by no more than 5% of –2.27 eV, making it still the highest interaction energy, agreeing with the distance of oxygen to the centroid in Table 4.

Taking CBS as the more accurate energy (with a few exceptions in the values as discussed in the preceding paragraph) in our current calculation, it is found that 6-311++G(2df,2pd) and cc-pVQZ have consistently produced interaction energies closer to CBS extrapolated values, as compared to other basis sets. For the size of the systems considered in this study, the wall time for the double-zeta basis sets completion is mostly under 2 h, while for triple zeta in the range of 8 h to 4 d, and the largest basis is roughly doubled that of triple zeta. Hence, if permissible, for future energetic calculations on amide adsorption, these two basis sets can be used, if the application of CBS scheme is not possible. Keep in mind that the interaction energy obtained will still be overestimation over the CBS extrapolated values. Larger basis sets, for example, cc-pV5Z or 6-311G++G(3df,3pd) would require larger memory requirements, rather than processing power. For geometry optimization of molecular clusters involving kaolinite, it is suggested to use triple-zeta basis sets [32]. As to the contradictory result reported before this, by comparing the strongest interaction energy of NMA- and AA-kaolinite, the CBS values shown in Table 6 generally show that NMA-kaolinite attaches more strongly to kaolinite than AA-kaolinite. Using the highest interaction energy at 6-311++G(2df,2pd) (–2.76 eV for NMA and –1.77 eV for AA), the difference in interaction energy is 0.45 eV.

Further analysis of the interactions between the amide molecules and the kaolinite surface is based on the electron density ρ at the bond critical point (BCP), as suggested by Emamian et al. [33]. The suggested formula of binding energy (BE), mentioned in Eq. (2), enables finding the contribution of hydrogen bonding to the interactions. The BCPs are calculated from the Multiwfn [28], and an example of the locations of BCPs from the Multiwfn is shown in Fig. 3. It was found that the electron densities at BCPs are insensitive to the basis sets used, whence only the hydrogen bonding energy using the largest basis sets is shown in Table 7.

$$\mathrm{BE} \approx -223.08 \times \rho(\mathrm{rBCP}) + 0.7423 \qquad (2)$$

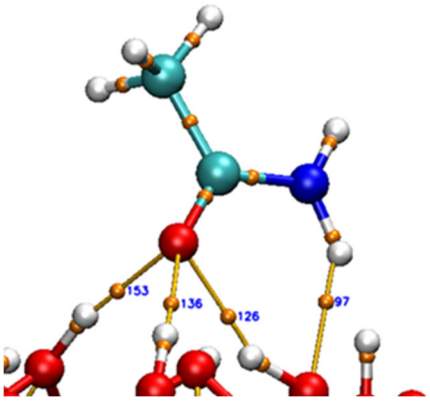

Fig 3. Locations of BCPs of hydrogen bonding between acetamide and Al–O surface. The figure is obtained using VMD [34].

Table 7. The binding energy (BE) of hydrogen bonding

System	BE (eV)
AA1	-1.14
AA2	-1.03
AA3	-1.20
NMA1	-0.66
NMA2	-1.06
NMA3	-0.96

As shown in Table 7, the hydrogen bonding to the interactions agrees with the distance to the centroid in Table 4. The shorter the distance, the higher the hydrogen bonding strength. The hydrogen bonding strengths in AA and NMA are similar (in the range –0.96 to –1.20 eV) when the distances are similar (2.90 to 3.04 Å). The lowest value at –0.66 eV is due to the large distance to the centroid. Compared to the reliable CBS values in Table 6, the hydrogen bonding is seen as a major component in the interaction energy and is important in stabilizing the system. The residue of the interaction energy might be due to the van der Waals or the dispersion energy.

■ CONCLUSION

The basis sets effects were studied systematically in our investigations of the adsorption of two simple amide molecules, acetamide and *N*-methyl-acetamide, on the Al–O surface of kaolinite. Although the decreasing pattern is obtained, using three basis sets in increasing size does not provide the convergence of the energies, be it with Pople or Dunning's basis sets. With the CBS extrapolation scheme, the extrapolated values are also needed to be assessed carefully, as the magnitude of increase in energy does not follow the increase in basis sets. Thus, comparison to the other basis of similar sizes is necessary to gauge the final extrapolated values. Even though the CBS value provides the limit of a functional at the basis set limit, in the case where it is not applicable, we found that the use of 6-311++G(2df,2pd) or cc-pVQZ is a good choice in studying the energetic components, with a certain degree of overestimation in magnitude. Finally, between AA and NMA, NMA is more strongly attached to the Al–O surface.

■ ACKNOWLEDGMENTS

The authors would like to express their sincere gratitude to Universiti Teknologi MARA (UiTM) and Universiti Sains Malaysia (USM) for their valuable support in the form of research funding and facilities.

■ REFERENCES

[1] Lehtola, S., 2021, Straightforward and accurate automatic auxiliary basis set generation for molecular calculations with atomic orbital basis sets, *J. Chem. Theory Comput.*, 17 (11), 6886–6900.

[2] Coşkun, M., and Ertürk, M., 2022, Double hyperbolic cosine basis sets for LCAO calculations, *Mol. Phys.*, 120 (17), e2109527.

[3] Morgante, P., and Peverati, R., 2020, The devil in the details: A tutorial review on some undervalued aspects of density functional theory calculations, *Int. J. Quantum Chem.*, 120 (18), e26332.

[4] Kirschner, K.N., Reith, D., and Heiden, W., 2020, The performance of Dunning, Jensen, and Karlsruhe basis sets on computing relative energies and geometries, *Soft Mater.*, 18 (2-3), 200–214.

[5] Akbudak, S., Uğur, G., Uğur, Ş., and Ocak, H.Y., 2019, Basis set convergence of binding energy with and without CP-correction utilizing PBEO method: A benchmark study of X_2 (X = Ge, As, Se, Sc, Ti, V, Cr, Mn, Co, Cu, Zn), *J. Theor. Comput. Chem.*, 18 (8), 1950034.

[6] Bowman, M.C., Zhang, B.Y., Morgan, W.J., and Schaefer, H.F., 2019, A remarkable case of basis set dependence: The false convergence patterns of the methyl anion, *Mol. Phys.*, 117 (9-12), 1069–1077.

[7] Myllys, N., Elm, J., and Kurtén, T., 2016, Density functional theory basis set convergence of sulfuric acid-containing molecular clusters, *Comput. Theor. Chem.*, 1098, 1–12.

[8] Jensen, F., 2023, Basis set extrapolation of vibrational frequencies, *J. Phys. Chem. A*, 127 (12), 2859–2863.

[9] Kraus, P., 2021, Extrapolating DFT toward the complete basis set limit: Lessons from the PBE family of functionals, *J. Chem. Theory Comput.*, 17 (9), 5651–5660.

[10] Pansini, F.N.N., Neto, A.C., and Varandas, A.J.C., 2016, Extrapolation of Hartree-Fock and multiconfiguration self-consistent-field energies to the complete basis set limit, *Theor. Chem. Acc.*, 135 (12), 261.

[11] Kupka, T., Buczek, A., Broda, M.A., Gajda, L., and Ignasiak, M., 2018, Convergence of nuclear magnetic shieldings and one-bond (1)J((BH)-B-11-

H-1) indirect spin-spin coupling constants in small boron molecules, *Magn. Reson. Chem.*, 56 (5), 338.

[12] Buczek, A., Kupka, T., Broda, M.A., and Żyła, A., 2016, Predicting the structure and vibrational frequencies of ethylene using harmonic and anharmonic approaches at the Kohn–Sham complete basis set limit, *J. Mol. Model.*, 22 (1), 42.

[13] Kitagawa, Y., Matsui, T., Yasuda, N., Hatake, H., Kawakami, T., Yamanaka, S., Nihei, M., Okumura, M., Oshio, H., and Yamaguchi, K., 2013, DFT calculations of effective exchange integrals at the complete basis set limit on oxo-vanadium ring complex, *Polyhedron*, 66, 97–101.

[14] Isegawa, M., Neese, F., and Pantazis, D.A., 2016, Ionization energies and aqueous redox potentials of organic molecules: Comparison of DFT, correlated ab Initio theory and pair natural orbital approaches, *J. Chem. Theory Comput.*, 12 (5), 2272–2284.

[15] Vasilyev, V., 2017, Online complete basis set limit extrapolation calculator, *Comput. Theor. Chem.*, 1115, 1–3.

[16] Sacchi, M., and Tamtögl, A., 2023, Water adsorption and dynamics on graphene and other 2D materials: Computational and experimental advances, *Adv. Phys.: X*, 8 (1), 2134051.

[17] Zhao, N., Tan, Y.X., Zhang, X., Zhen, Z.S., Song, Q.W., Ju, F., and Ling, H., 2023, Molecular insights on the adsorption of polycyclic aromatic hydrocarbons on soil clay minerals, *Environ. Eng. Sci.*, 40 (3), 105–113.

[18] Cheng, Q., Conejo, A.N., Wang, Y., Zhang, J., Zheng, A., and Liu, Z., 2023, Adsorption properties of hydrogen with iron oxides (FeO, Fe_2O_3): A ReaxFF molecular dynamics study, *Comput. Mater. Sci.*, 218, 111926.

[19] Piela, L., 2014, "Chapter 13 - Intermolecular Interactions" in *Ideas of Quantum Chemistry (Second Edition)*, Elsevier, Oxford, UK, 793–882.

[20] Grabowski, S.J., 2017, New type of halogen bond: Multivalent halogen interacting with π- and σ-electrons, *Molecules*, 22 (12), 2150.

[21] Dawley, M.M., Scott, A.M., Hill, F.C., Leszczynski, J., and Orlando, T.M., 2012, Adsorption of formamide on kaolinite surfaces: A combined infrared experimental and theoretical study, *J. Phys. Chem. C*, 116 (45), 23981–23991.

[22] Michalkova Scott, A., Dawley, M.M., Orlando, T.M., Hill, F.C., and Leszczynski, J., 2012, Theoretical study of the roles of Na^+ and water on the adsorption of formamide on kaolinite surfaces, *J. Phys. Chem. C*, 116 (45), 23992–24005.

[23] Song, K., Wang, X., Qian, P., Zhang, C., and Zhang, Q., 2013, Theoretical study of interaction of formamide with kaolinite, *Comput. Theor. Chem.*, 1020, 72–80.

[24] Song, K.H., Zhong, M.J., Wang, L., Li, Y., and Qian, P., 2014, Theoretical study of interaction of amide molecules with kaolinite, *Comput. Theor. Chem.*, 1050, 58–67.

[25] Bish, D.L., 1993, Rietveld refinement of the kaolinite structure at 1.5 K, *Clays Clay Miner.*, 41 (6), 738–744.

[26] Tunega, D., Haberhauer, G., Gerzabek, M.H., and Lischka, H., 2002, Theoretical study of adsorption sites on the (001) surfaces of 1:1 clay minerals, *Langmuir*, 18 (1), 139–147.

[27] Frisch, M.J., Trucks, G.W., Schlegel, H.B., Scuseria, G.E., Robb, M.A., Cheeseman, J.R., Scalmani, G., Barone, V., Petersson, G.A., Nakatsuji, H., Li, X., Caricato, M., Marenich, A., Bloino, J., Janesko, B.G., Gomperts, R., Mennucci, B., Hratchian, H.P., Ortiz, J.V., Izmaylov, A.F., Sonnenberg, J.L., Williams-Young, D., Ding, F., Lipparini, F., Egidi, F., Goings, J., Peng, B., Petrone, A., Henderson, T., Ranasinghe, D., Zakrzewski, V.G., Gao, J., Rega, N., Zheng, G., Liang, W., Hada, M., Ehara, M., Toyota, K., Fukuda, R., Hasegawa, J., Ishida, M., Nakajima, T., Honda, Y., Kitao, O., Nakai, H., Vreven, T., Throssell, K., Montgomery, Jr., J.A., Peralta, J.E., Ogliaro, F., Bearpark, M., Heyd, J.J., Brothers, E., Kudin, K.N., Staroverov, V.N., Keith, T., Kobayashi, R., Normand, J., Raghavachari, K., Rendell, A., Burant, J.C., Iyengar, S.S., Tomasi, J., Cossi, M., Millam, J.M., Klene, M., Adamo, C., Cammi, R., Ochterski,

J.W., Martin, R.L., Morokuma, K., Farkas, O., Foresman, J.B., and Fox, D.J., 2016, *Gaussian 09, Revision D.01*, Gaussian, Inc., Wallingford CT.

[28] Lu, T., and Chen, F., 2012, Multiwfn: A multifunctional wavefunction analyzer, *J. Comput. Chem.*, 33 (5), 580–592.

[29] Dennington, R., Keith, T.A., and Millam, J.M., 2016, *GaussView, Version 6.1*, Semichem Inc., Shawnee Mission, KS.

[30] Pettersen, E.F., Goddard, T.D., Huang, C.C., Meng, E.C., Couch, G.S., Croll, T.I., Morris, J.H., and Ferrin, T.E., 2021, UCSF ChimeraX: Structure visualization for researchers, educators, and developers, *Protein Sci.*, 30 (1), 70–82.

[31] Xiao, J., Zhao, Y.P., Fan, X., Cao, J.P., Kang, G.J., Zhao, W., and Wei, X.Y., 2017, Hydrogen bonding interactions between the organic oxygen/nitrogen monomers of lignite and water molecules: A DFT and AIM study, *Fuel Process. Technol.*, 168, 58–64.

[32] Nabil, N.N.A.M., and Ang, L.S., 2022, Selecting suitable functionals and basis sets on the study structural and adsorption of urea-kaolinite system using cluster method, *Indones. J. Chem.*, 22 (2), 361–373.

[33] Emamian, S., Lu, T., Kruse, H., and Emamian, H., 2019, Exploring nature and predicting strength of hydrogen bonds: A correlation analysis between atoms-in-molecules descriptors, binding energies, and energy components of symmetry-adapted perturbation theory, *J. Comput. Chem.*, 40 (32), 2868–2881.

[34] Humphrey, W., Dalke, A., and Schulten, K., 1996, VMD: Visual molecular dynamics, *J. Mol. Graphics*, 14 (1), 33–38.